5-14-2007

First THz and IR characterization of nanometer-scaled antenna-coupled InGaAs/InP Schottky-diode detectors for room temperature infrared imaging

Hooman Kazemi

Keisuke Shinohara

Gabor Nagy

Wonill Ha

Brian A. Lail

See next page for additional authors

Authors
Hooman Kazemi, Keisuke Shinohara, Gabor Nagy, Wonill Ha, Brian A. Lail, E. N. Grossman, Guy Zummo, William R. Folks, Javier Alda, and Glenn D. Boreman

First THz and IR characterization of nanometer-scaled antenna-coupled InGaAs/InP Schottky-diode detectors for room temperature infrared imaging*

H. Kazemi[1], K. Shinohara[1], G. Nagy[1], W. Ha[1], B. Lail[2], E. Grossman[3], G. Zummo[4], W. R. Folks[4], J. Alda[4], G. Boreman[4]

[1]Teledyne Scientific Company, Thousand Oaks, CA 91358-0085
[2]Dept. of Electrical and Computer Engineering, Florida Institute of Technology, Melbourne FL 32901
[3]National Institute of Standards and Technology (NIST), 325 Broadway, Boulder, CO 80305-3328
[4]CREOL, University of Central Florida, Orlando, FL 32816-2700

Abstract– **Nanometer high performance InP Schottky detectors are scaled to IR wavelengths. The increased cutoff frequency of the Schottky detector was accomplished by both reducing its capacitance to attofarad range and also by reducing the contact resistance. The Schottky detectors were fabricated on InGaAs/InP substrates with the doping level as high as 1 x 10^{19} cm^{-2}. The typical Schottky detector anode size was 0.1 x 1 μm^2. Planar broadband antennas were designed for LWIR wavelengths to couple the radiation into the nanometer size detector. Several different IR antenna designs were evaluated, including complimentary square spirals, bow ties and crossed dipoles. A 6 × 7 array of antenna-coupled Schottky detectors was characterized at DC, yielding a 20 KΩ zero-bias resistance and a responsivity of 6 A/W for the entire array. The arrays were characterized at 2.5 THz, as well as in the IR (3-5μm and 10.6 μm). The current results for polarization sensitivity confirm that an antenna-coupled mechanism is responsible for the measured responsivity with the highest value measured at the THz range.**

Index Terms— **Schottky diodes, zero-bias detectors, infrared rectification, responsivity, low-noise operation**

I. INTRODUCTION

Schottky diodes are one of the most widely used devices in the microwave and millimeter wave frequency range and are employed in circuits such as mixers, frequency multipliers, phase shifters and detectors [1]. Due to their ultra fast transport mechanism they are scalable to very high frequencies by reducing their physical contact area. GaAs and InP high performance Schottky diodes have been used extensively in the THz range. The advantage of using rectification as an operating device mechanism at IR wavelengths is the possible realization of such electronic systems as phased array radar. Novel components such as optical-electrical mixers (down conversion) and power generation with frequency multiplication become possible at LWIR range. Room temperature LWIR detection is also of great interest for high speed IR imagers. This could be achieved by using a Schottky diode as a detector coupled to an IR scaled antenna. The IR energy is collected from a pixel size area by the antenna and delivered as IR current to the detector. The detector performs the rectification and transfers the IR signal into a dc voltage which is subsequently recorded by the readout circuit. For greater nonlinearity of the detector, we see a higher dc signal output and a higher dynamic range. In recent years, antenna coupled IR detection has been demonstrated [2,3] and have shown polarization dependence, tunability and rapid time of response. In this paper we describe a novel method of using nano-scaled InP based Schottky contact diodes as detectors in the MWIR and LWIR bands. A variety of detector sizes were fabricated using nanometer T-gate technology to reduce the time constant of the sensors. Figure 1 shows a cross sectional view of ebeam defined photoresist template used for defining nanometer contacts on InP substrates. The detectors are antenna coupled through planar antennas such as spiral and slot arrays. Characterization of the antenna coupled detectors was carried out at 2.5 THz, and at 10.6 μm and 3-5 μm wavelengths.

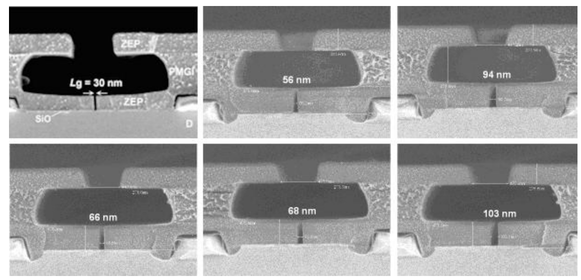

Figure 1- Cross sectional view of e-beam defined nano- scaled Schottky contacts from 30-100 nm gate lengths

II. DETECTOR FABRICATION

The nanoscaled detectors were fabricated on 4" InP wafers with the Schottky contact defined by the e-beam lithography technique. The epitaxial wafers had a low

* This Work is supported by DARPA MTO under MicroArray Antenna, Technology and Applications (MIATA) Program , Army Research Laboratory under the contract W911QX-04-C-0125 and Teledyne Scientific Company IR&D.

Infrared Technology and Applications XXXIII, edited by Bjørn F. Andresen, Gabor F. Fulop, Paul R. Norton,
Proc. of SPIE Vol. 6542, 65421J, (2007) · 0277-786X/07/$18 · doi: 10.1117/12.718887

sheet resistance material of 3 ohms/square for the ohmic layer. This layer was grown with a high level of Si doping using lattice matched InGaAs layer at 2×10^{19} cm^{-2}. The Schottky layer was Si doped at 1×10^{19} cm^{-2} and provided a semiconductor contact layer for the e-beam defined metal. The thickness of the ohmic and the Schottky layers were 300 nm and 100 nm respectively.

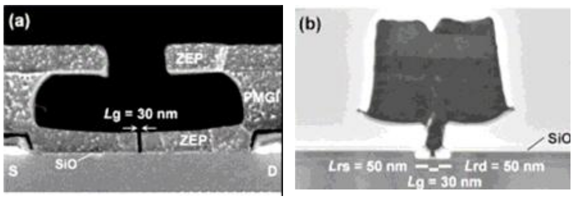

Figure 2- Cross sectional view of ebeam defined 30 nm InGaAs Schottky contacts with a controlled recess depth based on a InP sacrificial layer.

A 5-nm InP layer was added to the top of the Schottky layer to serve as a sacrificial layer with high etch selectivity during the Schottky contact formation. The first major fabrication process is the mesa isolation between each active device. This is performed using a wet chemical etch process. The low resistance ohmic contact (cathode) is formed with non-alloyed contact comprising of Ti/Pt/Au.

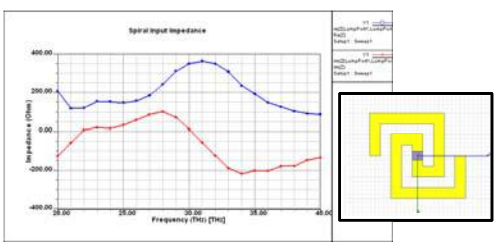

Figure 3 – Spiral IR antenna design.

A 20-nm-thick silicon oxide (SiO) layer is evaporated to improve resist adhesion, to define the gate footprint, and to also support the T-gate. A conventional tri-layer resist (ZEP/PMGI/ZEP) is used for e-beam lithography. Ebeam exposure is carried out with a beam current of 100 pA using a 50-keV JEOL EB tool. Figure 2(a) is a cross-sectional SEM image of a trilayer resist after development, showing an ultra-fine 30-nm-long gate-foot pattern with an overhang structure. The gate-foot pattern is then precisely replicated on the SiO layer by reactive ion etching (RIE) using CF_4 chemistry gas. Etching the sacrificial InP layer and stopping on the Schottky layer complete the gate recess process. A HCl and citric acid ($C_6H_8O_7$) based solution is used as an etch for this process to provide the needed selectivity between the layers. The lateral length of the recess is controlled by the etching time with the opening and effectively the metal dimension set by the dry etch dimension defined by the SiO layer. Figure 2(b) is a complete T-gate with an Lg of 30 nm and a lateral length of gate recess (Lrs = Lrd) of 50 nm. A middle part of the T-gate is made thick to increase mechanical strength as well as to decrease vertical resistance component of Rg.

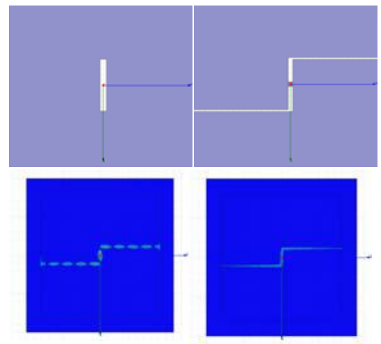

Figure 4-(a) Slot in solid ground plane, (b) slot with ground plane cuts for dc bias (c) 28.3 THz and (d) 2.5 THz field plots.

The planar antennas and the detectors were monolithically integrated on the wafer. The T-gate anode was extended to connect to the arm of the planar antenna. This was accomplished by extending the head of the T-gate to create an airbridge over the conductive mesa. At the feed point of the antenna one side was connected to the anode (T-gate) and the other was connected to the cathode as the ohmic contact. The gap at the feed point of the antenna is a design parameter and at IR is generally smaller than 5 μm. Due to this dimensional constraint, a considerable optimization of the fabrication process was undertaken to maintain yield and avoid short circuits between the antenna arms.

III. BROADBAND IR ANTENNA DESIGNS

Antenna-coupled response is achieved by placing the diode at the feed of a receiving antenna. THz and IR characterization was achieved with two principal antenna designs; (1) square spiral (figure 3), and (2) slot (figure 4). Equiangular spirals are examples of frequency-independent antennas, the result of a self-complementary geometry which can be fully described by angles [3]. The square spiral provides similar behavior with a geometry made of straight edges, which is preferred for lithographic fabrication. Microbolometer-coupled square spirals have been demonstrated at λ=10.6 μm [1]. The active region of a spiral design is approximated by the area enclosed by a one wavelength circumferential path about the center.

The lower and upper operating wavelengths are defined in terms of the inner and outer radii, respectively. Within the operating band, the excited currents form traveling waves on the arm. For long wavelengths, the active region includes the outer arms where reflections occur and the antenna ceases to be self-complementary. This gives rise to a characteristic zero in the input reactance and subsequent capacitive reactance which approaches zero as frequency increases, marking the beginning of the broad impedance bandwidth. Spiral antennas are circularly polarized. Therefore, antenna-coupled response may be identified through selective polarization illumination. It should be noted that both orthogonal circular polarization states might be received in a spiral array by alternating the orientation of individual elements. A square spiral as shown in Figure 3 was modeled and fabricated. Input impedance for a single-turn of 1.25 μm linewidth is shown. At λ=10.6 μm a >25% impedance bandwidth is achievable with a 300 Ω load. The radiation pattern is normal to the antenna plane, with half-power beamwidth (HPBW) 45^o in both planes.

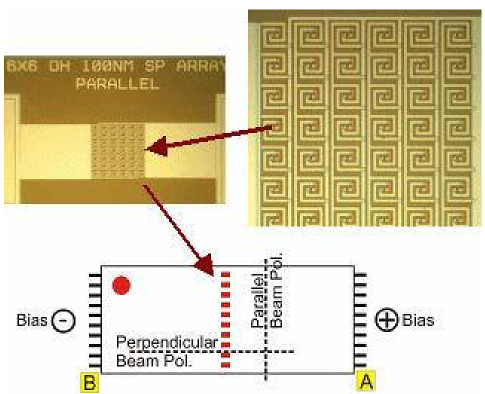

Figure 5. Pixel of 7 by 6 IR spiral antennas.

Slot-coupled response has been demonstrated at both millimeter and IR [2]. A slot design was developed for THz and IR characterization in this study. Figure 4 depicts an IR slot in a solid ground plane. The diode is placed across the midpoint where excited electric-field is peaked across the gap, and bias voltage is provided by cutting the ground plane in order to isolate the contacts. The configuration shown in Figure 4 was designed and fabricated. Nominal input impedance is 100 Ω, with HPBW > 75^o for test frequencies 2.5, 4.25, and 28.3 THz. The presence of cuts in the ground plane transforms the slot, a resonant structure, into a long slot that supports traveling-waves. A snapshot of field plots in the plane of the slot is shown in Figure 4 for both 28.3 THz and 2.5 THz. These fields propagate along the horizontal cuts. The vertical portion of the slot has a length that supports 10.6 μm excitation, while longer wavelengths excite fields extending along the horizontal cuts. Therefore, 28.3 THz response is preferential to horizontal polarization while the 2.5 THz excitation responds better to vertical polarization.

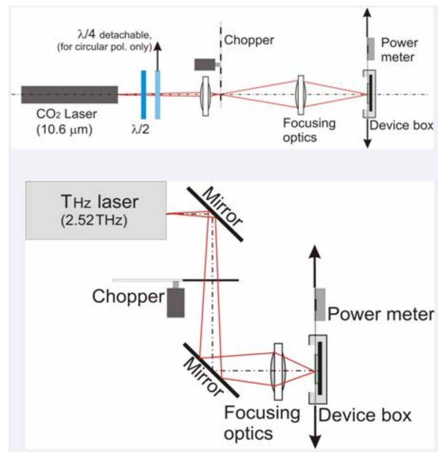

Figure 6. Sensor testing apparatus.

IV. DETECTOR CHARACTERIZATION

The antenna coupled detector arrays were fabricated both as a slot and a spiral arrays of 7 parallel columns by 6 series rows. The array chips were diced from the InP wafers and then mounted on the alumina carriers for characterization as shown in figure 5. The dc signal is collected and extended out of the array to large contacts. The dc current-voltage curves of the nanometer antenna coupled arrays were used to extract responsivity and dynamic diode resistance. The responsivity measured averaged at 6 A/W with a zero-bias resistance of 20 KΩ. Irradiance responsivity measurements were performed at λ = 10.6 μm, MWIR (3-5 μm), and the terahertz band. A CO2 gas laser, quartz halogen lamp and filter, and a tunable terahertz gas laser (2.5 THz) were used as sources. The source power apparent at

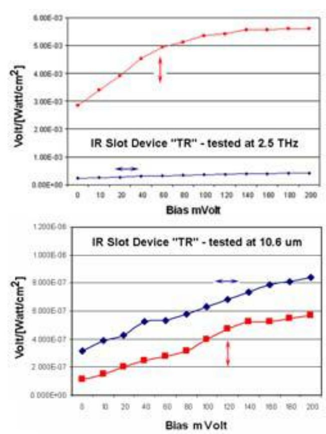

Figure 7. Polarization response for THz and LWIR.

the device was measured with a wide band heat-flow calorimeter. Appropriate collimation optics in combination with a low f/# focusing lens was used in all cases to focus power on the device as shown in figure 6. The device carrier was mounted on a precision xyz translation stage to allow fine positioning of the device with respect to the beam. Measurements were performed for both polarizations; parallel and perpendicular to the column of devices on the chip carrier, and also circular polarization for the 10.6 µm measurements. Switching between parallel and perpendicular orientation was achieved by manual rotation of the carrier or with a half-wave plate. Measurements were performed at twelve different bias points from 0 to 200 mV at all wavelengths.

Bias polarity was chosen for maximum signal as shown in figure 7. The THz data exhibits more than a 10:1 polarization ratio, while the LWIR data shows about a 2:1 polarization ratio. Device irradiance responsivity is reported in units of volts per watt per cm^2. Figure 7 represents the responsivity measurements at 2.5 THz and at 10.6 µm, in both vertical and horizontal polarizations. The slot-antenna-coupled diode had significant polarization-dependent response at 2.5 THz (> 10:1 maximum co-polarization/cross-polarization ratio). The response at 10.6 µm is also polarization dependent, but the contrast is not as strong (2:1 ratio). Ground-plane cuts provided a resonance mode for THz, although the slot antenna was designed for IR. The maximum THz polarization was perpendicular to the polarization for maximum IR response. It is also shown that the response is strongly affected by the bias voltage. This might be due to the increase in the non-linearity of the device junction with applied bias. Figure 8 shows the results of the responsivity as a function bias for THz, LWIR and MWIR wavelength for the spiral arrays. It is shown that the highest responsivity is achieved at the 2.5 THz and the lowest at the 10.6 µm while the 3-5 µm results slightly lower than the 2.5 THz. The mechanism of response for each wavelength might not be the same since there could be rectification, photovoltaic and photoconductive responses present. These effects might also have the opposite phase polarities and effectively cancel each other's responses. Further experiments are underway to establish the cause of the response and improve the responsivity by increasing the rectification mechanism and eliminate the photovoltaic and photoconductive responses.

V. Conclusion

Novel InP based Schottky contacts have been scaled to IR wavelengths. The nanometer Schottky contacts have been integrated with planar antennas such as spiral and slot structures. The fabrication process establishes a novel technique for integration of such detectors with planar antennas. The antenna designs have been optimized for operation in the LWIR region. Both slot and spiral arrays have been characterized at 2.5 THz frequency range and at 10.6 µm 3-5 µm wavelengths. At 2.5 THz the slot array shows a strong antenna coupled response that is explained by the slot antenna structure orientation. The responsivity results for the spiral array at three wavelengths show the highest response in the terahertz range followed by 3-5 µm and 10.6 µm. It is thought that there are various response mechanism present with rectification, photovoltaic and photoconductive being the main source of response. Further investigations are required to establish each mechanism and optimize the responsivity accordingly.

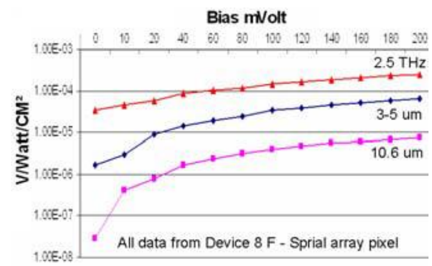

Figure 8. Comparison of irradiance responsivity for THz, LWIR, and MWIR.

VI. Acknowledgement

The authors would like to thank Ms. Lan Tran for her technical help and patience during the assembly process.

VII. References

[1] P. T. Siegel, "Terahertz Technology", IEEE, MTT, Vol., 50, No. 3, March 2002

[2] F.J. Gonzalez and G.D. Boreman, "Comparison of Dipole, Bowtie, Spiral and Log-periodic IR Antennas," Infrared Physics and Technology, Vol. 46, No. 5, pp. 418-428, June 2005.

[3] M. Abdel-Rahman, B. Lail and G. Boreman, "Dual-band Millimeter-wave/infrared Focal-plane Arrays," Microwave and Optical Technology Letters, Vol. 46, No. 1, July 2005.

[4] W.L. Stutzman, G.A. Thiele, Antenna Theory and Design, John Wiley & Sons, New York, 1998.